JETP Letters, Vol. 77, No. 10, 2003, pp. 592–597. Translated from Pis'ma v Zhurnal Éksperimental'noĭ i Teoreticheskoĭ Fiziki, Vol. 77, No. 10, 2003, pp. 696–701.

Anisotropy of Microwave Conductivity in the Superconducting and Normal States of $YBa_2Cu_3O_{7-x}$: 3D–2D Crossover

M. R. Trunin* and Yu. A. Nefedov

Institute of Solid State Physics, Russian Academy of Sciences, Chernogolovka, Moscow region, 142432 Russia

**e-mail: trunin@issp.ac.ru*

Received April 23, 2003

The imaginary parts of microwave conductivity σ'' ($T < T_c$) and resistivity $\rho(T) = 1/\sigma(T > T_c)$ along (σ''_{ab} and ρ_{ab}) and across (σ''_c and ρ_c) the cuprate *ab* planes of a $YBa_2Cu_3O_{7-x}$ crystal with the oxygen doping level x varying from 0.07 to 0.47 were measured in the temperature range $5 \le T \le 200$ K. In the superconducting state, the $\sigma''_{ab}(T)/\sigma''_{ab}(0)$ and $\sigma''_c(T)/\sigma''_c(0)$ curves coincide for an optimally doped ($x = 0.07$) crystal, but, with an increase in x, the slopes of the $\sigma''_c(T)/\sigma''_c(0)$ curves decrease noticeably at $T < T_c/3$, on the background of small changes happening to the $\sigma''_{ab}(T)/\sigma''_{ab}(0)$ curves. The two-dimensional (2D) transport along the *ab* planes in the normal state of $YBa_2Cu_3O_{7-x}$ is always metallic, but there is a crossover (at $x = 0.07$) from the Drude to hopping (at $x > 0.07$) conductivity along the c axis. This is confirmed both by the estimates of the lowest metallic and the highest tunneling conductivities along the c axis and by quantitative comparison of the measured $\rho_c(T)$ curves with the curves calculated in the polaron model of quasiparticle transport along the c axis. *© 2003 MAIK "Nauka/Interperiodica".*

PACS numbers: 74.25.Fy; 74.72.Bk

In recent years, growing interest has been shown in the evolution of transport properties of high-temperature superconductors (HTSCs) upon changing the level of doping with oxygen and other substitutional impurities or, in other words, upon changing the hole concentrations p per one copper atom in the CuO_2 plane. The p value and the superconducting transition temperature T_c in HTSC are related by the empirical formula [1] $T_c = T_{c,\max}[1 - 82.6(p - 0.16)^2]$.

A narrow region in the phase diagram of an optimally doped HTSC ($p \approx 0.16$) with maximal critical temperatures $T_c = T_{c,\max}$ has received most attention. In the normal state of an optimally doped HTSC, the resistivity $\rho_{ab}(T)$ in the cuprate *ab* planes increases linearly with temperature, $\Delta\rho_{ab}(T) \propto T$. The quantity $\rho_{ab}(T)$ is much smaller than the resistivity $\rho_c(T)$ in the perpendicular direction, which also has a metallic character (the derivatives of $\rho_{ab}(T)$ and $\rho_c(T)$ with respect to temperature are positive). The exception is provided by the most anisotropic HTSC compound Bi-2212 (the corresponding ratio is $\rho_c/\rho_{ab} \approx 10^5$ at $p \approx 0.16$), for which the resistivity $\rho_c(T)$ increases as T approaches T_c ($d\rho_c(T)/dT < 0$). This property of Bi-2212 agrees with the estimate of the lowest possible metallic conductivity in the c direction for anisotropic three-dimensional (3D) Fermi-liquid model [2]:

$$\sigma^{3D}_{c,\min} = \sqrt{\rho_{ab}/\rho_c}\, ne^2d^2/h, \tag{1}$$

where $n \approx 10^{21}$ cm^{-3} is the carrier concentration, d is the lattice constant along the c axis, and h is Planck's constant. In Bi-2212, the conductivity $\sigma_c = 1/\rho_c \ll \sigma^{3D}_{c,\min}$ at $T = T_c$, but, in other optimally doped HTSCs, $\sigma_c(T) > \sigma^{3D}_{c,\min}(T_c)$. The conductivity $\sigma_{c,\min}$ in Eq. (1) is lower than the two-dimensional Ioffe–Regel limiting value $\sigma_{IR} = e^2k_F/h$: $\sigma_{c,\min} \approx \sqrt{\rho_{ab}/\rho_c}\,\sigma_{IR}d/a \ll \sigma_{IR}$ ($a \approx 2\pi/k_F$ is the lattice constant in the CuO_2 plane), whereas $\sigma_{ab,\min} \approx \sigma_{IR}$ [2].

The ratio of the superconducting liquid densities in the cuprate planes and in the perpendicular direction serves as a measure of HTSC anisotropy in the superconducting state. This ratio equals $\sigma''_{ab}(0)/\sigma''_c(0) = \lambda_c^2(0)/\lambda_{ab}^2(0)$, where σ''_{ab} and σ''_c are the imaginary parts of the corresponding conductivities and λ_{ab} and λ_c are the microwave-field penetration depths for the currents flowing, respectively, in the *ab* planes and perpendicularly to them. It is well known that, in high-quality optimally doped HTSC single crystals, $\Delta\lambda_{ab}(T) \propto T$ at $T < T_c/3$, and this experimental fact suggests a $d_{x^2-y^2}$ symmetry of the order parameter in them [3]. There is no agreement in the literature about the low-temperature behavior of $\Delta\lambda_c(T)$. Both the linear dependence $\Delta\lambda_c(T) \propto T$ at $T < T_c/3$ [4–6] and the quadratic dependence [7] have been observed for the most studied $YBa_2Cu_3O_{6.95}$ ($T_c \approx 93$ K) single crystals.

Annealing temperatures, doping parameters, and characteristics of the superconducting and normal states of $YBa_2Cu_3O_{7-x}$

Annealing temperature T, °C	Critical temperature T_c, °C	Doping parameters		λ values at $T = 0$		$\Delta\lambda_c(T) \propto T^{\alpha}$	λ_c/λ_{ab} at $T = 0$	$\sqrt{\rho_c/\rho_{ab}}$ at $T = 200$ K
		p	x	λ_{ab}, nm	λ_c, μm	α		
500	92	0.15	0.07	152	1.55	1.0	10	11
520	80	0.12	0.26	170	3.0	1.1	18	18
550	70	0.105	0.33	178	5.2	1.2	29	16
600	57	0.092	0.40	190	6.9	1.3	36	16
720	41	0.078	0.47	198	16.3	1.8	83	35

A broad region of pseudogap states arising in the HTSC phase diagram at concentrations $p < 0.16$ has been studied to a much lesser extent. It follows from the measurements of dynamic susceptibility of oriented HTSC powders at $T < T_c$ [8] that, at $T \longrightarrow 0$, the slopes of $\sigma''_c(T)/\sigma''_c(0)$ for $\sigma''_{ab}(T)/\sigma''_{ab}(0)$. The nonmetallic behavior of resistivity $\rho_c(T)$ as T approaches T_c, the deviations from the linear dependence $\Delta\rho_{ab}(T) \propto T$, and a dramatic increase in the ratio ρ_c/ρ_{ab} with decreasing concentration p are common properties of underdoped HTSCs in their normal state. Although many theoretical models have been proposed for the explanation of these properties, none of them describes in full measure the evolution of the $\sigma''_{ab}(T)$, $\sigma''_c(T)$, $\rho_{ab}(T)$, and $\rho_c(T)$ curves over a wide range of concentrations and temperatures. The transport mechanism along the c axis has also not been established, and, in particular, it still remains unclear whether it can be metallic (of the Drude type) or whether the conductivity for any p is caused by the quasiparticle tunneling between the cuprate layers with scattering both within the layers and between them.

In this work, the anisotropy and evolution of temperature dependences of the conductivity components of $YBa_2Cu_3O_{7-x}$ with oxygen doping in the range $0.07 \le x \le 0.47$ were measured and the measurement results were analyzed. The crystal was grown in a $BaZrO_3$ crucible and had a rectilinear shape with sizes $1.6 \times 0.4 \times 0.1$ mm. Measurements were performed at a frequency $\omega/2\pi = 9.4$ GHz and temperatures $5 \le T \le 200$ K. The oxygen content in the sample changed through the controlled annealing in air at different temperatures $T \ge 500$°C (listed in the table). Measurements of the conductivity anisotropy were carried out for each of the five crystal states, in which the superconducting transition width, according to the susceptibility measurements at a frequency of 100 kHz, was 0.1 K in the optimally doped ($x = 0.07$) state and increased with x to reach 4 K at $x = 0.47$. The superconducting transition temperatures were $T_c = 92$, 80, 70, 57, and 41 K. The full cycle of microwave studies included (i) measurements of the temperature dependences of the Q value and the frequency shift for a superconducting niobium cavity with crystal samples in two, transverse and longitudinal, orientations about the microwave magnetic field; (ii) determination of the surface resistance $R_{ab}(T)$, reactance $X_{ab}(T)$, and conductivity $\sigma_{ab}(T)$ of the cuprate planes in the normal and superconducting states from the measurements in the first orientation; and (iii) determination of $\sigma_c(T)$, $X_c(T)$, and $R_c(T)$ using the data obtained for the longitudinal orientation. The entire measurement procedure for the optimally doped $YBa_2Cu_3O_{6.95}$ crystal is described in detail in [6]. The temperature dependences of the components of surface impedance of $YBa_2Cu_3O_{7-x}$ at different x were reported in our short communication [9].

The $\sigma''_{ab}(T)/\sigma''_{ab}(0)$ (light symbols) and $\sigma''_c(T)/\sigma''_c(0)$ (dark symbols) curves at $T \le T_c$ are presented in Fig. 1 for the $YBa_2Cu_3O_{7-x}$ crystal in the states with $T_c = 92$, 70, and 41 K. The field penetration depths $\lambda_{ab}(0)$ and $\lambda_c(0)$ at $T = 0$ are also given in the table. The overall temperature behavior of the $\sigma''_{ab}(T)/\sigma''_{ab}(0)$ curves changes only slightly upon varying p. A distinctive feature of the optimally doped $YBa_2Cu_3O_{6.93}$ state is that the temperature dependences $\sigma''_{ab}(T)/\sigma''_{ab}(0)$ and $\sigma''_c(T)/\sigma''_c(0)$ coincide to a good accuracy. This fact can be rigorously explained only in the theory of linear response of an anisotropic 3D superconductor [8]. As p decreases, the $\sigma''_c(T)/\sigma''_c(0)$ dependence at $T < T_c/3$ becomes noticeably weaker than $\sigma''_{ab}(T)/\sigma''_{ab}(0)$.

The model proposed in [10] is most suitable for a comparison with the experimental data of our work. In this model, the following contributions to the quasiparticle transport along the c axis in the superconducting and normal HTSC states are considered: (a) direct hopping between the cuprate planes and (b) hopping with inelastic scattering from impurities located between the planes. The conductivity within the cuprate planes is assumed to be of the Drude type:

$$\sigma_{ab} = \frac{e^2 \nu_{2D} D_{ab}}{d} = \frac{n_{2D} e^2 \tau}{md}, \qquad (2)$$

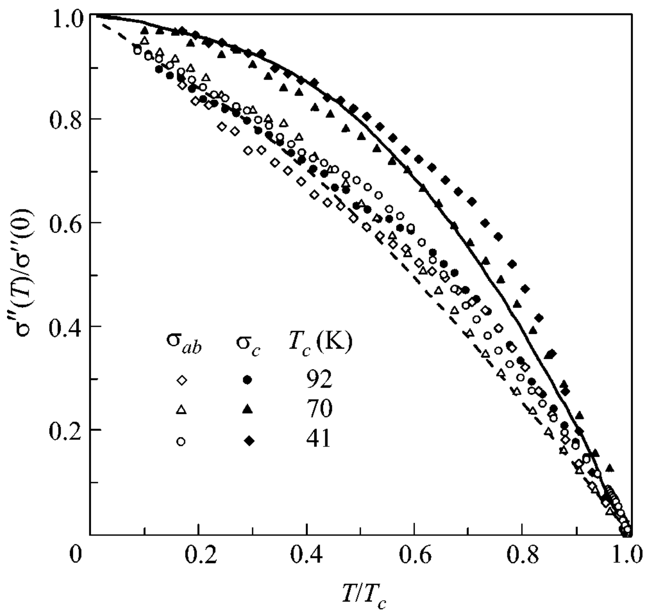

Fig. 1. The $\sigma''_{ab}(T)/\sigma''_{ab}(0)$ (light symbols) and $\sigma''_c(T)/\sigma''_c(0)$ (dark symbols) measured curves for three states of a $YBa_2Cu_3O_{7-x}$ crystal with T_c = 92, 70, and 41 K. The solid and dashed lines correspond, respectively, to the $\sigma''_c(T)/\sigma''_c(0)$ and $\sigma''_{ab}(T)/\sigma''_{ab}(0)$ dependences calculated in [10] for oxygen-deficient $YBa_2Cu_3O_{7-x}$.

where $\nu_{2D} = m/\pi\hbar^2$ is the two-dimensional density of states per unit area and $D_{ab} = v_F^2\tau/2$, v_F, τ, and $n_{2D} = k_F^2/2\pi$ are the diffusion coefficient, Fermi velocity, relaxation time, and two-dimensional quasiparticle density in the *ab* plane, respectively. The total Hamiltonian of the electron system in model [10] is the sum $\sum_m H_m$ of the Hamiltonians of individual (m) CuO_2 layers and the interplane Hamiltonian $H_\perp$, which is assumed to be small compared to $\sum_m H_m$. As a result, the second-order perturbative quasiparticle transport between the neighboring weakly bonded layers proves to be analogous to the tunneling through the *SIS* junction at $T < T_c$ and through the *NIN* junction at $T > T_c$. In this case, the *ab* component of electron momentum is conserved in process (a) (mirror tunneling) and is not conserved in process (b) (diffuse tunneling) [11].

The calculations of the anisotropy of the superconducting HTSC state were carried out in [10] using the BCS model with a *d*-symmetry order parameter in the CuO_2 layers. The $\sigma''_c(T)/\sigma''_c(0)$ curve numerically calculated with allowance for both processes (a) and (b) is shown in Fig. 1 by the solid line and the same for $\sigma''_{ab}(T)/\sigma''_{ab}(0)$ is shown by the dashed line. A comparison with the experimental data obtained at $T < T_c/2$ for $YBa_2Cu_3O_{7-x}$ with an oxygen deficiency $x > 0.07$ clearly demonstrates that the slopes of the $\sigma''_c(T)/\sigma''_c(0)$ curves strongly decrease with increasing x, while the $\sigma''_{ab}(T)/\sigma''_{ab}(0)$ curves change only slightly. The fact that the experimental curves at $T > T_c/2$ are steeper than the theoretical ones may be caused by the strong electron–phonon interaction [3], which was not taken into account in [10]. The dashed line in Fig. 1 coincides also with the $\sigma''_c(T)/\sigma''_c(0)$ curve calculated in [10] for the case where there is no diffuse tunneling (b) and the remaining mirror-tunneling regime (a) along the c axis becomes identical with the transport along c in an anisotropic 3D superconductor. This exceptional situation corresponds to the optimally doped $YBa_2Cu_3O_{6.93}$.

The real and imaginary parts of the surface impedance measured for the $YBa_2Cu_3O_{7-x}$ crystal at $T > T_c$ coincided with each other; i.e., $R_{ab}(T) = X_{ab}(T)$ and $R_c(T) = X_c(T)$ for each x from the table [9]. Because of this, the resistivities $\rho_{ab}(T)$ and $\rho_c(T)$ were derived from $R_{ab}(T)$ and $R_c(T)$ using the standard formulas for the normal skin effect: $\rho_{ab}(T) = 2R_{ab}^2(T)/\omega\mu_0$ and $\rho_c(T) = 2R_c^2(T)/\omega\mu_0$. The evolution of the $\rho_{ab}(T)$ and $\rho_c(T)$ curves with changing x is shown in Fig. 2 for the temperature range $T_c < T \le 200$ K, and the $(\rho_c/\rho_{ab})^{1/2}$ values at $T = 200$ K are given in the last column of the table. The $\rho_{ab}(T)$ and $\rho_c(T)$ dependences have a metallic character only in optimally doped $YBa_2Cu_3O_{6.93}$, and the ρ_c/ρ_{ab} ratio approximately corresponds to the anisotropy of charge-carrier effective masses $m_c/m_{ab} = \lambda_c^2(0)/\lambda_{ab}^2(0)$ in a pure 3D London superconductor, to which $YBa_2Cu_3O_{6.93}$ belongs. In all other $YBa_2Cu_3O_{7-x}$ states with a lower hole concentration, the resistivity $\rho_c(T)$ increases with temperature decreasing, demonstrating the nonmetallic behavior. In Fig. 3, the experimental $\sigma_c(T)$ dependences are compared with the $\sigma^{3D}_{c,\min}$ values calculated by Eq. (1) for three states of the $YBa_2Cu_3O_{7-x}$ crystal: T_c = 92 K (dashed line), T_c = 70 K (dotted line), and T_c = 41 K (dot-and-dash line). Over the entire temperature interval, the $YBa_2Cu_3O_{6.93}$ conductivity along c is the only one that exceeds the minimal metallic value of $\sigma^{3D}_{c,\min}$.

Thus, it is natural to assume that, as in the case of the superconducting state of $YBa_2Cu_3O_{7-x}$, a small decrease in the carrier concentration from its optimal level in the normal state leads to a crossover from the 3D metallic conduction to the 2D Drude conduction in the CuO_2 layers and tunneling conduction between the layers (3D–2D crossover). To analyze this assumption, it is convenient to again use model [10]. If $t_\perp$ is the hop-

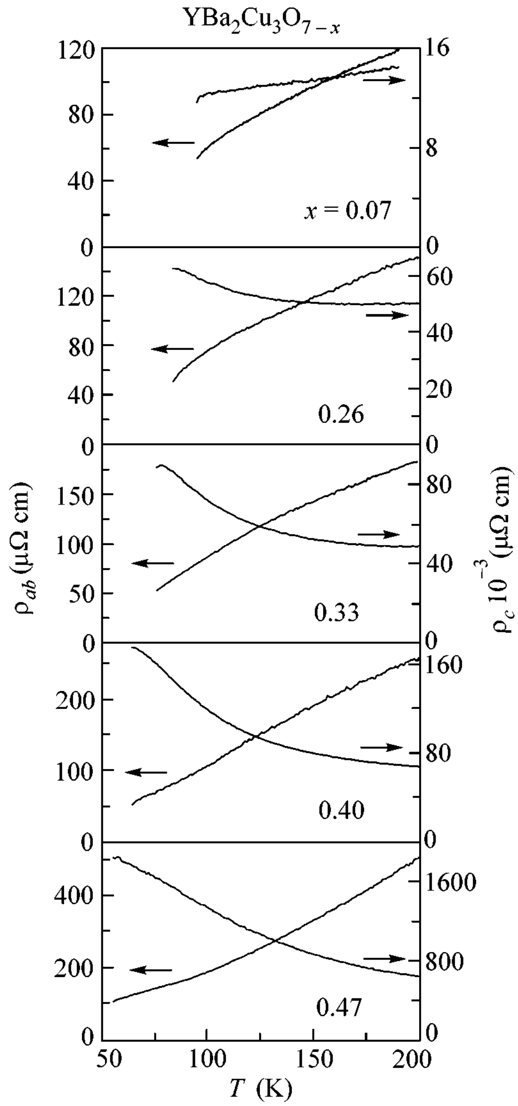

Fig. 2. Evolution of the $\rho_{ab}(T)$ and $\rho_c(T)$ dependences measured for $YBa_2Cu_3O_{7-x}$ with differing oxygen content.

ping matrix element, the quasiparticle conductivity along c in process (a) will be [10–13]

$$\sigma_c^{\mathrm{dir}} = 2e^2\tau\nu_{2D}\left(\frac{t_\perp}{\hbar}\right)^2 = 4\sigma_{ab}\left(\frac{t_\perp d}{\hbar v_F}\right)^2, \tag{3}$$

where $2\tau(t_\perp/\hbar)^2$ is the direct-tunneling rate between the neighboring CuO_2 planes and σ_{ab} is the conductivity along these planes (Eq. (2)). In this case, the characteristic hopping time $\hbar/t_\perp$ appreciably exceeds the in-plane relaxation time τ [11]: $\hbar/t_\perp \gg \tau$. In the reverse limit $\hbar/t_\perp \ll \tau$, the conductivity is of the Drude type in all directions, as in the case of an anisotropic 3D metal. The crossover occurs when $\hbar/t_\perp \approx \tau$. At this point, the tunneling conductivity along c (Eq. (3)) reaches its maximum $\sigma_{c,\max}^{\mathrm{dir}} = 2\sigma_{IR}\sqrt{\rho_{ab}/\rho_c}$, which is approximately equal to the minimal metallic conductivity $\sigma_{c,\max}^{3D}$ given by Eq. (1). In the case of diffuse quasiparticle tunneling (processes (b)) in model [10], the conductivity along the c axis equals [11, 14]

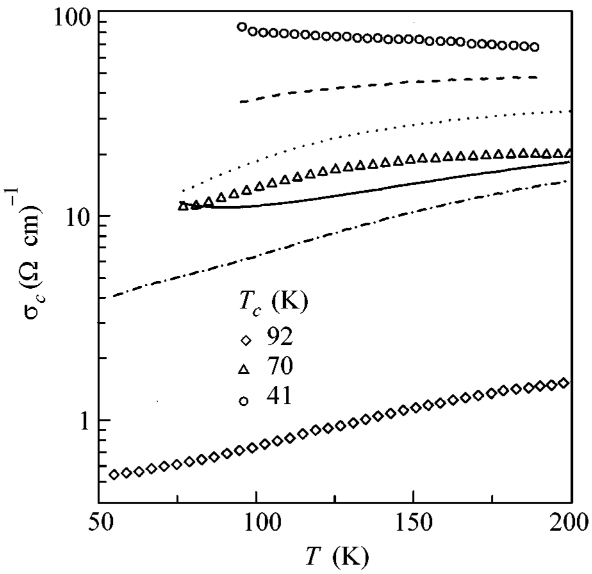

Fig. 3. Symbols correspond to the experimental $\sigma_c(T)$ dependences for three $YBa_2Cu_3O_{7-x}$ states with T_c = 92, 70, and 41 K. The dashed, dotted, and dot-and-dash lines are for the corresponding $\sigma_{c,\min}^{3D}(T)$ values obtained from Eq. (1) using the measured $\rho_{ab}(T)$ and $\rho_c(T)$ presented in Fig. 2. The solid line corresponds to $\sigma_c(T)$ calculated for $YBa_2Cu_3O_{6.67}$ by the formulas given in [10].

$$\sigma_c^{\mathrm{diff}} = \frac{e^2\nu_{2D}D_c}{d} = \frac{e^2\nu_{2D}d}{\tau_c}, \tag{4}$$

where $D_c = d^2\tau_c$ is the diffusion coefficient and $1/\tau_c$ is the scattering probability between the cuprate planes. As in the preceding case, we find that $\sigma_{c,\max}^{\mathrm{diff}} = \sigma_{IR}\sqrt{\rho_{ab}/\rho_c} \approx \sigma_{c,\min}^{3D}$ for $\tau_c \approx \tau$, and, using Eqs. (2) and (4), we arrive at the following alternative form of the criterion for a 3D–2D crossover:

$$\sigma_{c,\max}\sigma_{ab} \approx \frac{n_{2D}}{\pi}\left(\frac{e^2}{\hbar}\right)^2. \tag{5}$$

From Eq. (5) it follows that, at $n_{2D} = n/d \approx 10^{14}$ cm^{-2}, the 3D–2D crossover occurs upon reaching the value $\rho_c\rho_{ab} \approx 10^{-6}$ $(\Omega$ cm$)^2$. Returning to the data in Fig. 2, we make sure that the product $\rho_c\rho_{ab} \lesssim 10^{-6}$ $(\Omega$ cm$)^2$ only at $x = 0.07$, thereby substantiating the applicability of the anisotropic 3D Fermi-liquid model for explaining the properties of optimally doped $YBa_2Cu_3O_{6.93}$.

Equations (3) and (4) account for the basically different temperature dependences of the conductivity

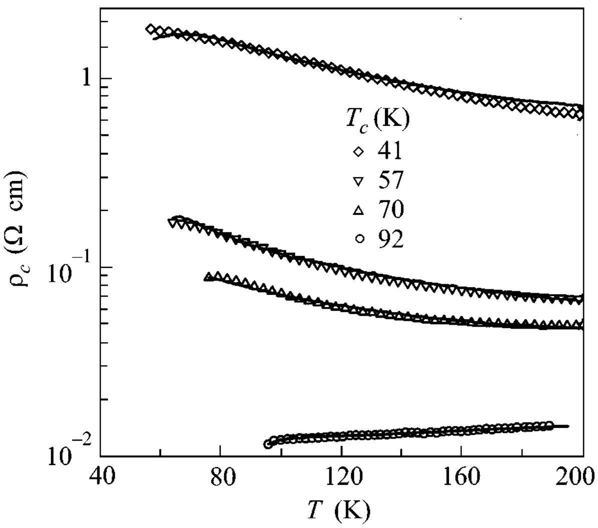

Fig. 4. Comparison of the (symbols) experimental and (solid lines) calculated (by formula (6)) $\rho_c(T)$ dependences for $YBa_2Cu_3O_{7-x}$.

along the c axis at $T \geq T_c$; for the direct tunneling, $\sigma_c^{\text{dir}}(T) \propto \sigma_{ab}(T)$ increases with increasing $\tau(T)$ as T approaches T_c, whereas $\sigma_c^{\text{diff}}(T)$ decreases with increasing $\tau_c(T)$. According to model [10], the total conductivity σ_c along the c axis is the sum of conductivities caused by each of the above-mentioned processes ((a) and (b)). Near the T_c temperatures, σ_c^{diff} is mainly due to the quasiparticle scattering from the impurities located between the cuprate planes and, hence, is independent of T, because the phonon contribution to σ_c^{diff} is frozen out. Quite the reverse, the phonon contribution becomes dominant at $T \gg T_c$. As a result, the temperature dependence of the conductivity $\sigma_c(T)$ takes an approximate form, $A/T + C + BT$ (A, B, and C are independent of T), that does not describe the experimental data; an example of $\sigma_c(T)$ calculated by the formulas given in [10] is shown by the solid line in Fig. 3 for the $YBa_2Cu_3O_{6.67}$ sample.

However, all $\rho_c(T)$ dependences shown in Fig. 2 can be described by the c-transport model that was recently proposed in [15]. Contrary to [10], where the electron–phonon effects appeared in the second-order of the perturbation theory, the model Hamiltonian [15] includes them through the canonical transformation [16], after which the interplane quasiparticle tunneling can be considered as a perturbation of the originally strongly coupled electron–phonon system. This approach applies if $\epsilon_F \gg \omega_0 \gg t_\perp$, where ϵ_F is the Fermi energy and ω_0 is the characteristic phonon energy. Both inequalities are fulfilled for the layered anisotropic HTSCs, in which, according to [15], an electron moving in the c direction is enveloped by a large number of phonons to form polaron [17] that only weakly affects the transverse ab transport. For the Einstein spectrum of c-polarized phonons, one has

$$\rho_c(T) \propto \rho_{ab}(T)\frac{\exp[g^2\tanh(\omega_0/4T)]}{\sqrt{\sinh(\omega_0/2T)}}, \qquad (6)$$

where g ($g > 1$) is the parameter characterizing the electron–phonon coupling strength. The comparison of the experimental data (symbols) with the $\rho_c(T)$ dependences calculated by Eq. (6) (solid lines) is demonstrated in Fig. 4. In the calculations, the data given for $\rho_{ab}(T)$ in Fig. 2 were used. The parameter g was almost identical ($g \approx 3$) for all curves in Fig. 4, and ω_0 increased from 110 K (75 cm^{-1}) to 310 K (215 cm^{-1}) upon decreasing the oxygen content ($7 - x$) in $YBa_2Cu_3O_{7-x}$ from 6.93 to 6.53. It seems not surprising that the anomalies of the optical c conductivity were observed for a $YBa_2Cu_3O_{7-x}$ crystal with oxygen deficiency just in the indicated range of frequencies ω_0 [18].

In summary, the anisotropy of microwave conductivity was measured for a $YBa_2Cu_3O_{7-x}$ crystal in which the hole concentration p was varied in the range $0.08 \leq p \leq 0.15$. An analysis of the temperature dependences of the imaginary parts of the conductivity tensor $\hat{\sigma}''(T)$ in the superconducting state and the resistivity $\hat{\rho}(T)$ in the normal state indicates that optimally doped $YBa_2Cu_3O_{6.93}$ is a three-dimensional anisotropic metal. A decrease in the carrier concentration leads to a crossover from the Drude-type to hopping conduction along the c axis. In order to quantitatively describe the evolution of the $\sigma_c''(T)$ and $\rho_c(T)$ dependences with changing p, the effects of strong electron–phonon interaction must be taken into account.

We are grateful to V.F. Gantmakher and A.F. Shevchun for helpful discussions. This work was supported by the Russian Foundation for Basic Research, project nos. 03-02-16812, 03-02-06386, and 02-02-08004.

REFERENCES

1. J. L. Tallon, C. Bernhard, H. Shaked, *et al.*, Phys. Rev. B **51**, 12911 (1995).
2. Y. B. Xie, Phys. Rev. B **45**, 11375 (1992).
3. M. R. Trunin and A. A. Golubov, in *Spectroscopy of High-T_c Superconductors. A Theoretical View* (Taylor and Francis, London, 2003), p. 159.
4. J. Mao, D. H. Wu, J. L. Peng, *et al.*, Phys. Rev. B **51**, 3316 (1995).
5. H. Srikanth, Z. Zhai, S. Sridhar, *et al.*, J. Phys. Chem. Solids **59**, 2105 (1998).
6. Yu. A. Nefyodov, M. R. Trunin, A. A. Zhohov, *et al.*, Phys. Rev. B **67**, 144504 (2003).
7. A. Hosseini, S. Kamal, D. A. Bonn, *et al.*, Phys. Rev. Lett. **81**, 1298 (1998).

8. T. Xiang, C. Panagapoulos, and J. R. Cooper, Int. J. Mod. Phys. B **12**, 1007 (1998).
9. Yu. A. Nefyodov and M. R. Trunin, Physica C (Amsterdam) (2003) (in press).
10. R. J. Radtke, V. N. Kostur, and K. Levin, Phys. Rev. B **53**, R522 (1996); R. J. Radtke and K. Levin, Physica C (Amsterdam) **250**, 282 (1995); R. J. Rojo and K. Levin, Phys. Rev. B **48**, 16861 (1993).
11. M. Turlakov and A. J. Legget, Phys. Rev. B **63**, 064518 (2001).
12. N. Kumar and A. M. Jayannavar, Phys. Rev. B **45**, 5001 (1992).
13. L. B. Ioffe, A. I. Larkin, A. A. Varlamov, *et al.*, Phys. Rev. B **47**, 8936 (1993).
14. M. J. Graf, D. Rainer, and J. A. Sauls, Phys. Rev. B **47**, 12089 (1993).
15. A. F. Ho and A. J. Schofield, cond-mat/0211675.
16. I. G. Lang and Yu. A. Firsov, Zh. Éksp. Teor. Fiz. **43**, 1843 (1962) [Sov. Phys. JETP **16**, 1301 (1962)]; Zh. Éksp. Teor. Fiz. **45**, 378 (1963) [Sov. Phys. JETP **18**, 262 (1963)].
17. T. Holstein, Ann. Phys. (N.Y.) **8**, 343 (1959).
18. T. Timusk and B. Statt, Rep. Prog. Phys. **62**, 61 (1999).

Translated by V. Sakun